Failure Analysis of Deployable Thin-Shell Space Structures Using Refined One-Dimensional Finite Elements

Failure Analysis of Deployable Thin-Shell Space Structures Using Refined One-Dimensional Finite Elements

Daniele SCANO[1,a], Riccardo Augello[1,b], Erasmo CARRERA[1,c], Francesco LATINI[2,d] and Marco PETROLO[1,e *]

[1]MUL2 Lab, Department of Mechanical and Aerospace Engineering, Corso Duca degli Abruzzi 24, 10129, Torino, Italy

[2]Agenzia Spaziale Italiana, Via del Politecnico snc, 00133, Roma, Italy

[a]daniele.scano@polito.it, [b]riccardo.augello@polito.it, [c]erasmo.carrera@polito.it, [d]francesco.latini@asi.it, [e]marco.petrolo@polito.it

Keywords: Ultra-Thin Structures; One-Dimensional Refined Model; Carrera Unified Formulation; Failure Analysis

Abstract. This study investigates the failure of ultra-thin deployable composite structures. The analysis focuses on a laminated tape spring composed of three layers of glass fibre and carbon fibre reinforced polymers, subjected to opposing bending moments at its ends. The Carrera Unified Formulation (CUF) is employed for the numerical analysis within a geometrically nonlinear framework. This approach enables the accurate evaluation of the complete three-dimensional (3D) stress state at each equilibrium configuration. The Hashin 3D criterion is then applied to compute failure indices, allowing for the identification of critical points along the nonlinear equilibrium path. The results conclusively identify the mid-span section as the most critical region, with matrix-dominated failure modes being predominant.

Introduction

Deployable structures have gained prominence in space engineering due to their ability to reduce significantly mass, volume, and cost [1]. Typically fabricated from thin or ultra-thin materials, these structures are extensively used in applications such as satellite antennas [2]. Tape springs represent the most common type of deployable boom. While traditionally metallic, recent designs increasingly employ carbon fibre-reinforced plastic (CFRP) to achieve superior stiffness-to-mass ratios. These structures demand advanced analyses due to their nonlinear mechanical behaviour, including large deformations coupled with local and global instabilities, which can produce damages [3, 4]. Material nonlinearities present additional complexities, particularly when modelling composite or elastomeric components, where an accurate failure prediction is crucial and due to their propensity for multifaceted failure modes, making high-fidelity modelling both essential and challenging.

This study focuses on the accurate evaluation of three-dimensional (3D) stress fields and the failure mechanisms in space deployable structures by calculating the failure indices within the geometrical nonlinear framework. This study employs the one-dimensional version of Carrera Unified Formulation (CUF) [5, 6] for the structural modelling. CUF framework decomposes the three-dimensional displacement field into axial and cross-sectional components, enabling the implementation of higher-order theories that accurately capture cross-sectional deformation patterns. Specifically, Lagrange polynomial expansions are utilized to represent the kinematics. This refined beam formulation provides significant computational advantages over conventional 2D and 3D finite element approaches, particularly in terms of solution efficiency. The methodology maintains 3D solution accuracy while substantially reducing computational costs.

Materials Research Proceedings 69 (2026) 1210-1214 https://doi.org/10.21741/9781644904251-208

CUF has been recently adopted for calculating the nonlinear behaviour of deployable space structures [7, 8].

This paper is organized as follows: (a) Section *Methodology* introduces the principles of CUF in the nonlinear scenario; (b) Section *Numerical Results* presents the main outcomes; and (c) Section *Conclusions* summarizes the key findings of the study.

Methodology

According to the CUF, the 3D displacement field can be expressed in the following unified form:

$$\mathbf{u}(x,y,z) = F_\tau(x,z)\mathbf{u}_\tau, \qquad \tau = 1,2,\dots,M \tag{1}$$

where $\mathbf{u}$ denotes the displacement vector with components defined in the global reference system (x,y,z). $F_\tau\,(x,z)$ represent the cross-sectional functions in-plane coordinates (x,z), τ is the summation index, and M is the number of terms used in the cross-sectional displacement expansion. In the present work, quadratic Lagrange polynomials (L9) are adopted to approximate the kinematic field; further details can be found in [5]. The use of Lagrange polynomials enables the discretization of complex cross-sectional geometries.

To approximate the displacement field along the beam axis, the Finite Element Method (FEM) is employed. Thus, the displacement vector $\mathbf{u}_\tau(y)$ may be now expressed as:

$$\mathbf{u}(x,y,z) = N_i(y)F_\tau(x,z)\mathbf{u}_{\tau i}, \qquad i = 1,2,\dots,N_n \tag{2}$$

where $N_i(y)$ denotes the i-th one-dimensional shape function, i indicates summation, and N_n is the number of finite element nodes per element, whereas $\mathbf{u}_{\tau i}$ is the vector of nodal parameters. In this formulation, one-dimensional finite Lagrangian elements are used along the y-axis.

Finally, the stress $\boldsymbol{\sigma}$ and strain $\boldsymbol{\epsilon}$ components are expressed in vectorial form as:

$$\boldsymbol{\sigma} = \left\{\sigma_{xx}\ \sigma_{yy}\ \sigma_{zz}\ \sigma_{yz}\ \sigma_{xz}\ \sigma_{xy}\right\}^T, \quad \boldsymbol{\epsilon} = \left\{\epsilon_{xx}\ \epsilon_{yy}\ \epsilon_{zz}\ \epsilon_{yz}\ \epsilon_{xz}\ \epsilon_{xy}\right\}^T \tag{3}$$

Regarding the geometric relations, the Green–Lagrange nonlinear strain components can be written as

$$\boldsymbol{\epsilon} = \boldsymbol{\epsilon}_l + \boldsymbol{\epsilon}_{nl} = (\mathbf{b}_l + \mathbf{b}_{nl})\mathbf{u} \tag{4}$$

where $\boldsymbol{\epsilon}_l$ and $\boldsymbol{\epsilon}_{nl}$ denote the linear and nonlinear strain components, respectively. The 6×3 linear and nonlinear differential operators, $\mathbf{b}_l$ and $\mathbf{b}_{nl}$, are defined in detail in [9]. As far as the constitutive relation is concerned, linear elastic structures are considered in this work. Consequently, the constitutive relation reads as:

$$\boldsymbol{\sigma}^k = \mathbf{C}^k\boldsymbol{\epsilon}^k \tag{5}$$

where $\mathbf{C}^k$ is the material elastic matrix of the k-th layer, whose explicit form can be found in [5].

In this study, the 3D Hashin failure criterion [10] is employed to assess material failure. This criterion identifies the predominant failure mode at the ply level based on the local stress state. Four distinct failure indices are considered: Fiber Tension (FT), Fiber Compression (FC), Matrix Tension (MT), and Matrix Compression (MC).

Numerical results

The analysed tape spring has a length of L = 577 (mm), a thickness of t = 80 (ìm), a radius of r = 11.25 (mm), and a subtended angle of α = 90°, see Fig. 1. The structure is simply supported and subjected to two applied moments at its ends. The boom consists of three layers made of Carbon

Fiber (CF) and Glass Fiber Plain Weave (GFPW), as shown in Fig. 1 and detailed in Tables 1 and 2, [11]. Its stacking sequence is [±45GFPW/0CF/±45GFPW]°.

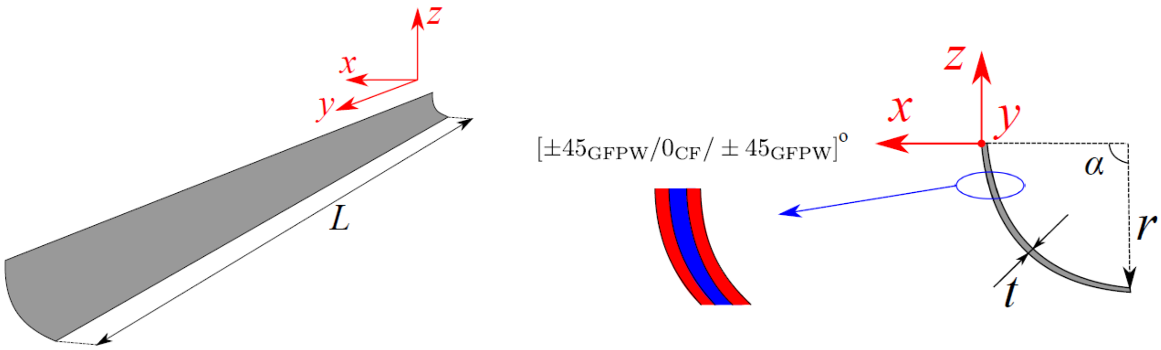

Figure 1: Geometrical details and stacking sequence of the tape-spring boom.

Table 1: Material characteristics of the tape-spring.

	E_1(GPa)	E_2(GPa)	G_{12}(GPa)	ν_{12}(-)	t(μm)
CF	128	6.5	7.6	0.32	
GFPW	23.8	23.8	3.3	0.17	

Table 2: Strength parameters for CF and GFPW in the tape-spring. Values in (MPa).

	X_T	X_C	Y_T	Y_C	S_{XY}	S_{XZ}	S_{XZ}
CF	2700	1650	55	225	100	100	32.26
GFPW	452.37	312.37	452.37	312.69	69.76	69.76	44.83

The structural model developed within CUF framework discretizes the cross-section into 30 L9 subdomains, enabling a piecewise parabolic approximation of the cross-sectional displacement field. Along the beam axis, two linear and eighteen cubic finite elements are employed, resulting in a total of 25,137 degrees of freedom (DOFs).

Figure 2 shows the equilibrium curve as a function of the angle θ, with the definitions of θ and the moment M provided for completeness. Point C (at θ = 6.8°) marks the equilibrium state where the MC failure index reaches a critical value. A detailed distribution of the MC failure index at the equilibrium configuration C is provided in Fig. 3 (a). The plot clearly illustrates the variation of each failure index across the laminate's thickness at the mid-span. Fig. 3 (b) makes a comparison between configurations C and D.

Finally, Table 3 summarizes the maximum values of the four failure indices at the location of peak stress concentration for equilibrium states A, B, C, and D (see Fig. 2), along with their corresponding angles θ. All four failure indices reach their maximum values at the mid-span section, even though at distinct locations through the thickness. Specifically, the critical points for FT, MT, and MC are located within the GFWP layers, whereas the critical point for FC lies in the CF layer.

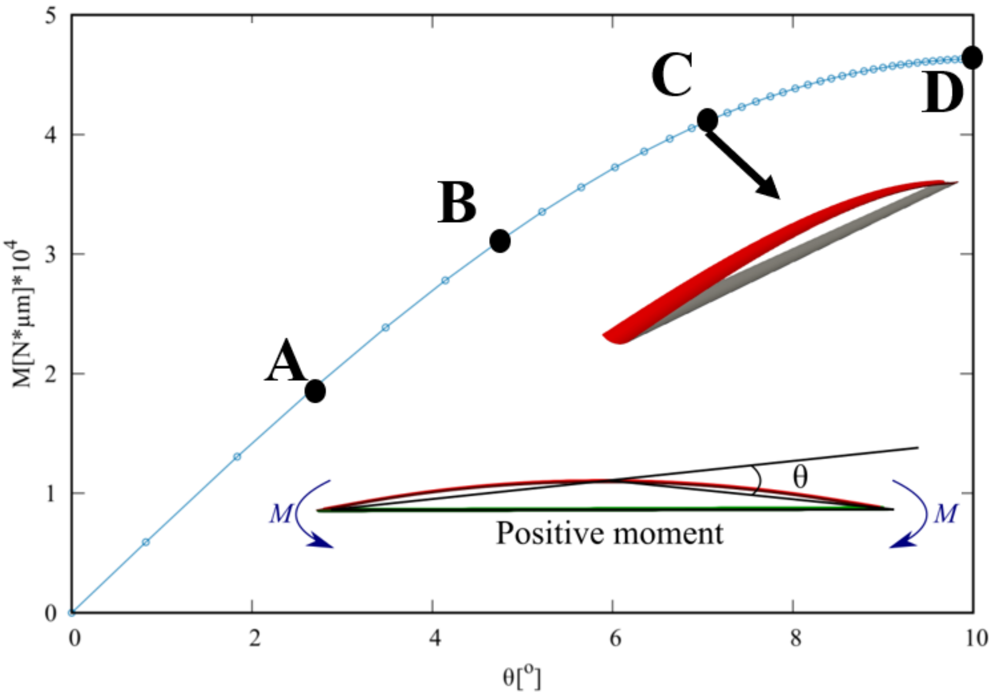

Figure 2: Equilibrium curve for the tape-spring boom.

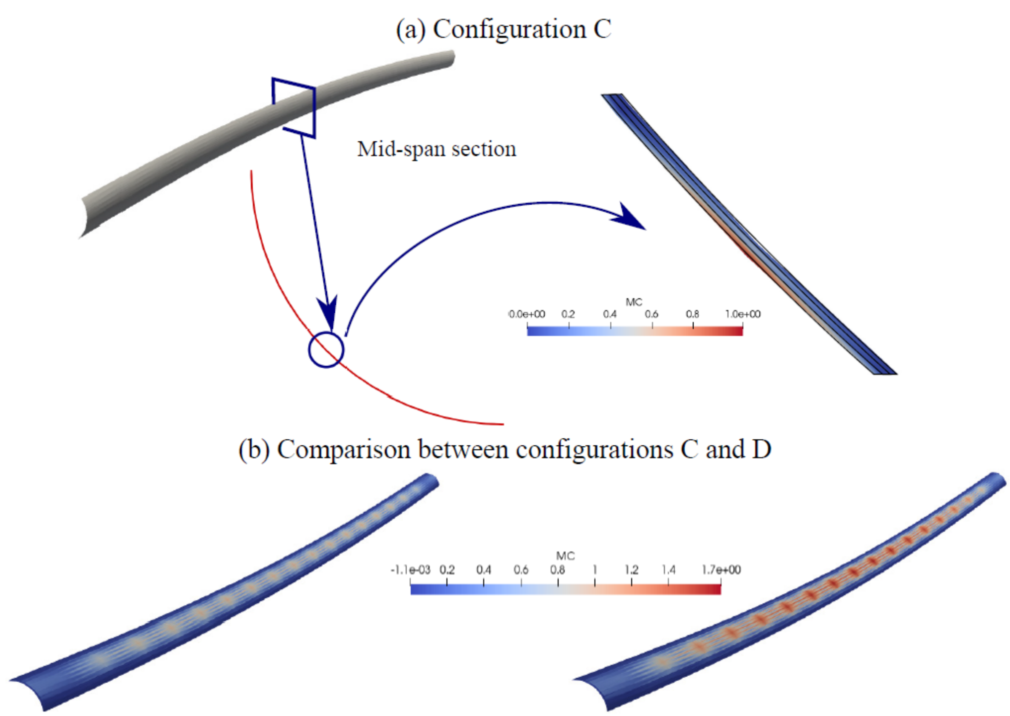

Figure 3: Failure indices for the equilibrium states C and D.

The results indicate that the structure may be susceptible to damage initiation even at relatively low angles of deformation. Among the considered failure indices, FT and FC, and MT are the least critical, whereas MC is significantly higher. The MC index, in particular, exhibits the most severe values, confirming it as the dominant failure mechanism. This analysis further reveals that the GFWP layers are the most prone to damage. Notably, the critical values for MC are reached during the nonlinear regime of the structural response.

Materials Research Proceedings 69 (2026) 1210-1214 https://doi.org/10.21741/9781644904251-208

Table 3: Failure indices for equilibrium points A, B, C, and D. (The locations are given in mm).

Configuration	θ[°]	FT (-0.0125,L/2,0)	FC (-3.51,L/2,-8.34)	MT (-4.22,L/2,8.94)	MC (-0.0125,L/2,-8.37)
A	2.7	0.000	0.000	0.010	0.16
B	4.7	0.002	0.000	0.026	0.44
C	6.8	0.006	0.002	0.031	1.03
D	9.9	0.009	0.002	0.050	1.69

Conclusions

This work has investigated the nonlinear behaviour of a tape-spring boom using a one-dimensional CUF framework. The Hashin 3D failure criterion was employed to assess the structure's failure state at various equilibrium points. It is important to note that the current model assumes a pristine, linear-elastic material response and does not incorporate damage progression. This simplification, the results clearly identify the mid-span region as the most critical area. Furthermore, the GFRP layers are identified as the most susceptible to damage initiation. Future work will focus on extending this analysis to include progressive failure modelling to accurately simulate damage initiation and evolution.

Acknowledgments

This study was carried out within the DISPCOMP funded by the Italian Space Agency, ASI, under contract n. 2024-38.I.0.

References

[1] P.A. Warren, Foldable member. U.S. Patent, 6: B1. (2002).
[2] F. Royer, S. Pellegrino, Ultralight ladder-type coilable space structures. In: 2018 AIAA Spacecraft Structures Conference, page 1200, 2018. https://doi.org/10.2514/6.2018-1200
[3] H.M.Y.C. Mallikarachchi, S. Pellegrino, Design of Ultrathin Composite Self-Deployable Booms, J. Spacecr. Rockets 51 (2014) 1811-1821. https://doi.org/10.2514/1.A32815
[4] K. Ubamanyu, D. Ghedalia, A.D. Hasanyan, S. Pellegrino. Experimental Study of Time dependent Failure of High Strain Composites. In: AIAA Scitech 2020 Forum, Orlando, FL, 6-10 January 2020. https://doi.org/10.2514/6.2020-0207
[5] E. Carrera, M. Cinefra, M. Petrolo, E. Zappino, Finite Element Analysis of Structures Through Unified Formulation, Wiley, Amsterdam, 2014. https://doi.org/10.1002/9781118536643
[6] D. Scano, E. Carrera, M. Petrolo, Use of the 3D Equilibrium Equations in the Free-Edge Analyses for Laminated Structures with the Variable Kinematics Approach, Aerotec. Missili Spaz. 103 (2024) 179-195. https://doi.org/10.1007/s42496-023-00177-2
[7] R. Augello, A. Pagani, E. Carrera, R. Masia, Virtual testing of folding and deployment of composite ultrathin tape spring hinges via unified 2D shell models. In: 73rd International Astronautical Congress (IAC), Paris, France, 18-22 September 2022.
[8] R. Augello, A. Pagani, E. Carrera, D.A. Iannotta, Stress and Failure Onset Analysis of Thin Composite Deployables by Global/Local Approach, AIAA J. 60 (2022) 5954-5966. https://doi.org/10.2514/1.J061899
[9] A. Pagani and E. Carrera, Unified formulation of geometrically nonlinear refined beam theories, Mech. Adv. Mater. Struct. 25 (2018) 15–31. https://doi.org/10.1080/15376494.2016.1232458
[10] Z. Hashin, Failure criteria for unidirectional fiber composites, J. Appl. Mech. 47 (1980) 329-334. https://doi.org/10.1115/1.3153664
[11] C. Leclerc, S. Pellegrino, Nonlinear elastic buckling of ultra-thin coilable booms, Int. J. Solids Struct. 202 (2020) 45–56. https://doi.org/10.1016/j.ijsolstr.2020.06.042